MARCH 06 2013

Plenum window insertion loss in the presence of a line source—A scale model study

Y. G. Tong; S. K. Tang

J. Acoust. Soc. Am. 133, 1458–1467 (2013)
https://doi.org/10.1121/1.4788996

Plenum window insertion loss in the presence of a line source—A scale model study

Y. G. Tong and S. K. Tang[a)]
Department of Building Services Engineering, The Hong Kong Polytechnic University, Hong Kong, China

(Received 6 January 2011; revised 26 December 2012; accepted 7 January 2013)

The acoustical insertion losses of plenum windows installed on a building facade in the presence of a non-parallel line source are studied by using a 1:4 scaled down model in a semi-anechoic chamber in the present investigation. Two types of insertion losses, weighted by the normalized traffic noise spectrum (from the 100 Hz to 5000 Hz one-third octave bands), are defined with different references. The first one is for the case where the orientation of the building facade relative to the line source is fixed. The reference case is the opened window having the same orientation angle as the plenum window. The maximum and minimum insertion losses under this condition across the orientations tested are found to be around 14 dB and 5 dB, respectively. The other is the opposite situation where such orientation is allowed to change because of practical purposes and the reference for this condition is the opened window with its width span parallel to the line source. The corresponding maximum and minimum insertion losses are found to be around 18 dB and 8 dB, respectively. There are evidences showing that the lower order plenum acoustic modes are responsible for the relatively high low frequency insertion loss.
 [http://dx.doi.org/10.1121/1.4788996]

PACS number(s): 43.50.Gf, 43.55.Ti [LMW] Pages: 1458–1467

I. INTRODUCTION

The rapid development and population growth in cities have resulted in many residential buildings being built close to ground transportation networks. Noise from road vehicles therefore has become one of the major forms of pollution affecting the sustainability of the society and the daily life of the citizens. The results of a recent survey suggests that over one-seventh of the Hong Kong population are living in areas with traffic noise level higher than the statutory limit of 70 dBA.[1] The quest for an effective sound mitigation method is one of the top priorities of the Hong Kong local authority.

Noise barriers and noise enclosures[2] are some options which can only be efficiently applied in new developments where land availability is not a big constraint. In built-up areas or in urban re-development projects where the usable land areas are usually very much limited, the building facades could be the only means for the acoustical protection against traffic noise. Balconies are proved to be inefficient screening devices in the high-rise environment.[3] The double and triple glazed windows can offer good sound insulation,[4] and their low frequency performance can also be improved using the active control technique.[5] However, this is done at the expense of indoor air quality unless mechanical ventilation is installed. Under the modern sustainability concept, the use of mechanical ventilation is not desirable as it will incur extra energy consumption. Natural ventilation has become an increasingly important consideration in modern residential building design.[6] Facade devices which can provide a high sound insulation but can allow for natural ventilation are attractive solutions at least to the Hong Kong urban noise problem. This forms the main objective of the present study.

A kind of ventilation window, which is basically an elongated version of the plenum applied to duct noise control,[7] has been proposed for use as an alternative solution to the traffic noise and aircraft noise intrusion problem.[8,9] This plenum structure provides insertion loss and at the same time allows some extents of air movement across it. Ford and Kerry[10] measured the sound insulation across double glazing windows with small openings in a reverberant environment (random incidence). They found that such windows can offer an acoustical protection about 10 dBA higher than the single glazing ones. Kang and Brocklesby[11] investigated the use of micro-perforated membrane inside the plenum window. They showed that the plenum windows of the right dimensions lined with micro-perforated panels could produce an acoustical protection better than closing a single glazing window. There are sufficient evidences that the plenum windows can be useful in tackling traffic noise problem in a densely populated high-rise city.

In the present study, the acoustical performance of the plenum windows is investigated in detail through scale model experiments carried out inside a semi-anechoic environment. The effect of window orientation relative to the sound source, which is assumed to be an incoherent line source in practice,[12] is also examined in detail. It is hoped that the present results can provide a more detailed picture on the acoustical benefit of using the plenum windows in practice.

II. EXPERIMENTAL SETUP

All the experiments in the present study were carried out inside a semi-anechoic testing chamber whose workable size was 5 m by 5 m by 4 m (height). The reverberation time

a)Author to whom correspondence should be addressed. Electronic mail: shiu-keung.tang@polyu.edu.hk

 0001-4966/2013/133(3)/1458/10/$30.00

of this semi-anechoic chamber was less than 0.2 s at frequencies above the 200 Hz one-third octave band and was about 0.5 s within the 100 Hz one-third octave band. This condition is more realistic than the reverberant one adopted by Ford and Kerry[10] as it is very rare to have a random incidence sound field in practical applications.

A. The scale model and the noise source

A 1:4 scale down model was adopted in the present study (Fig. 1). It was basically a small reverberation box made of 18 mm thick varnished plywood boards with no parallel internal surfaces. The widths and heights of the plenum windows were fixed at 500 mm (L) and 250 mm, respectively. Perspex plates of 3 mm thickness were used to simulate the glass panes of the full size plenum windows. The width of the plenum window opening w and the separation between the Perspex plates, which is hereinafter referred to as the plenum depth, d, varied from 50 mm to 250 mm and from 50 mm to 100 mm, respectively. The plenum window sill was fixed at 500 mm above the testing chamber floor throughout the present study. Details of the scale model rig configuration and dimensions are given in Fig. 1.

The reverberation times inside the reverberation box, which is hereinafter referred to as receiver chamber, are important in later calculation and were measured in the first place. The reverberation times at 12 randomly chosen locations inside the receiver chamber were measured using the DIRAC system in the 1:4 scale model mode with the MLS signal.[13] A two-inch aperture loudspeaker acted as the sound source for this measurement. In the rest of the paper, all frequencies are scaled back to the full scale plenum window case in order to avoid confusion.

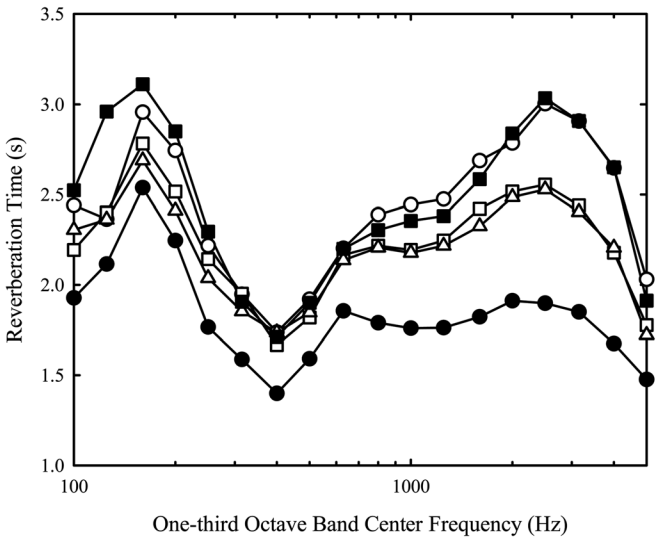

FIG. 2. Average reverberation times measured inside receiver chamber. $w/L = 0.1$ (open circle); $w/L = 0.25$ (open square); $w/L = 0.5$ (open triangle); opened window (closed circle); closed window (closed square). $d/L = 0.1$.

Figure 2 illustrates the average reverberation times measured inside the receiver chamber with different window openings w. The chamber was very reverberant over the on-third octave frequency bands from 100 Hz to 5000 Hz, which corresponded to that of the traffic noise in practice.[14] The standard deviations of the measured reverberation times were less than 0.3 s and thus are not presented. The reverberation times were also basically independent of the plenum window depth d (not shown here).

Six 1/4 in. microphones (Brüel & Kjær 4951) spanned over the internal volume of the receiver chamber were used to measure the average sound pressure level inside the receiver

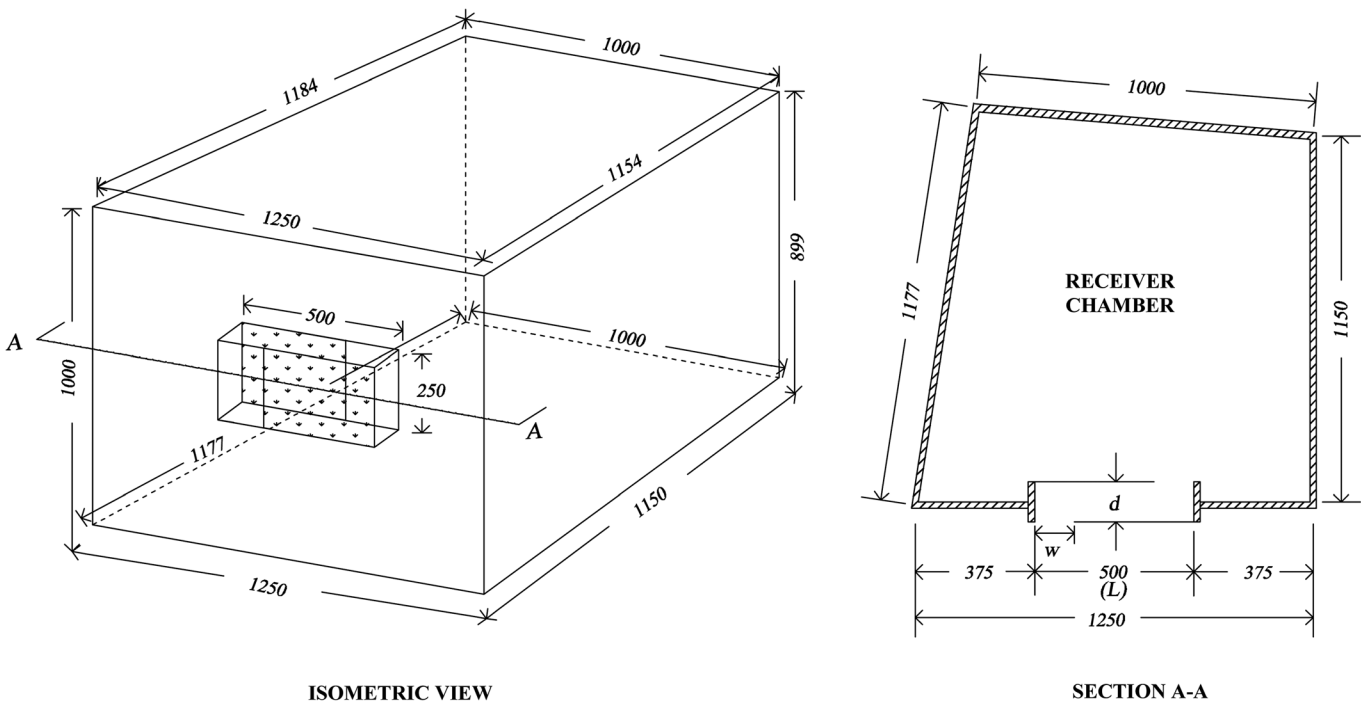

FIG. 1. Experimental model setup, its dimensions (in mm) and the nomenclature adopted.

chamber, while another six microphones of the same type were located externally in front of the plenum window to measure the average sound levels outside the receiver chamber. The present setting of receiver chamber measurement is in-line with those employed in insertion loss measurement, for instance, ISO140-3[15] and Kang.[16] The sound transmission class of the experimental model under the closed window condition, assuming the majority of sound was transmitted into the receiver chamber through the front panel where the window was installed, was measured to be 24. One can notice later from the experimental results that the sound leakage into the receiver chamber from locations other than the plenum window was not important.

The line source used in the present experiment consisted of twenty-five 6 in. aperture loudspeakers aligned in a linear array of ~5 m in length. The sound pressure level over the span of the plenum window was uniform when the latter was directly facing the line source. White noise signals were fed into the power amplifier which drove the loudspeakers. The output of the power amplifier was kept constant and was monitored through the present investigation.

B. Measurement procedure

The model was placed at 3 m away from the center of the loudspeaker array. The vertical centerline of the plenum window was chosen to be the axis about which the scale model was rotated for the study of the source orientation effects on the plenum window acoustical performance (Fig. 3). The orientation angle θ of 0° represents the case where the plenum window is directly facing the sound source. During the measurements, the angle θ was varied in an interval of 10°.

The data acquisition system employed in the present study was the Brüel & Kjær 3560D PULSE system, which recorded the noise signals from the 12 microphones (six inside and six outside the receiver chamber) and the power amplifier output simultaneously with a sampling rate of 65 536 samples per second per channel. The PULSE system also calculated the one-third octave band spectra. The air temperature and relative humidity inside the test room were maintained at 26 °C and 55%, respectively, throughout the measurements. Each measurement lasted for 30 s and the measurement repeatability, which was obtained from three individual measurements for each experimental setting, was within ±0.3 dB. The results presented later are the corresponding averages.

Since one of the major objectives of the present study is to estimate the acoustical protection of the plenum window in the presence of traffic noise, the normalized traffic noise spectrum depicted in the standard EN 1793-3[14] has to be applied. This normalized noise spectrum has very often been used in the estimation of the acoustical benefit in the presence of traffic noise in term of a single rating (for instance, Garai and Guidorzi[17] and Buratti[18]). In the present study, the acoustical performance of the plenum window, which is referred as the insertion loss, *IL*, is defined as the difference between the average noise levels, *SPL*, inside the receiver chamber and those of the opened window case (as the reference case). Since the reverberation times inside the receiver chamber did change with the window opening width, the effect of room constant is included in the calculation of the noise reduction:

$$R_i = SPL_{i,test} - SPL_{i,ref} - 10\log_{10}\left(\frac{RC_{i,ref}}{RC_{i,test}}\right) \tag{1}$$

and

$$IL = -10\log_{10}\left(\sum_{i=1}^{18} 10^{0.1(N_i - R_i)} \Big/ \sum_{i=1}^{18} 10^{0.1N_i}\right), \tag{2}$$

where i represents the ith one-third octave band (from 100 Hz to 5 kHz), RC the room constant, N the normalized

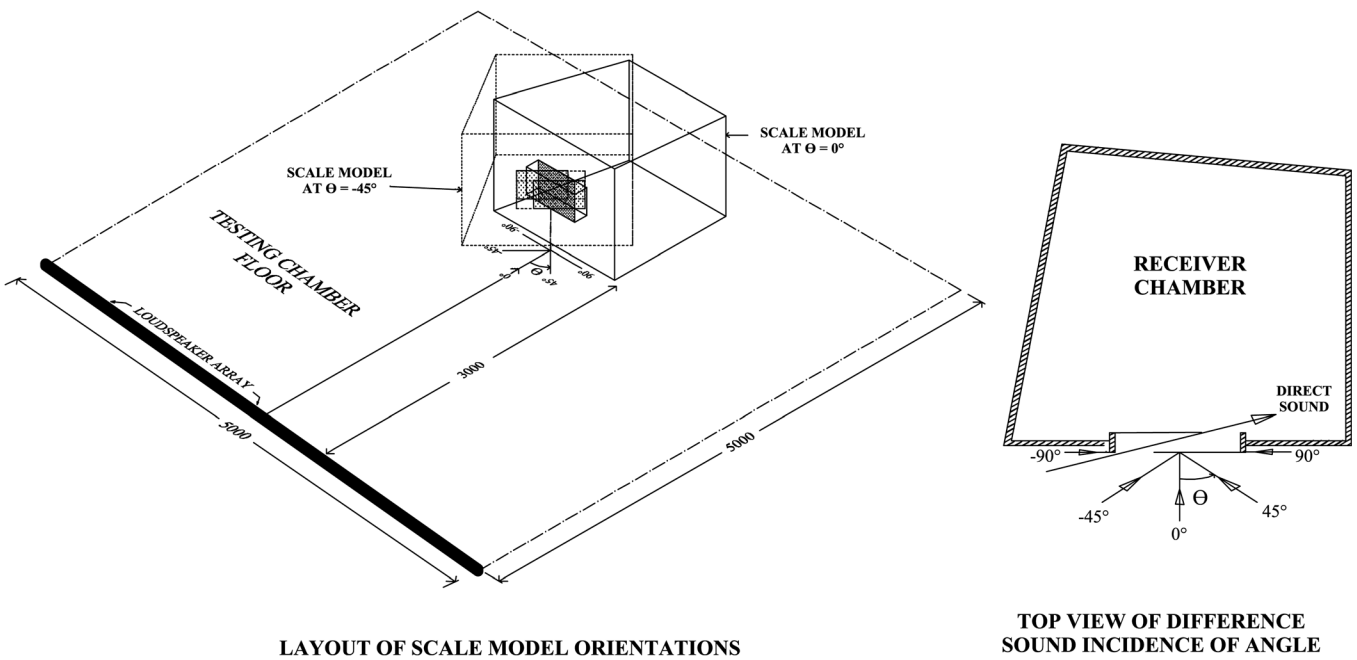

FIG. 3. Definition of orientation angle θ.

traffic noise band level and the suffices *ref* and *test* denote data obtained in the reference case and with the window installed, respectively.

Before moving into the next section, it is worthwhile to point out though the measurement uncertainty due to measurement system and its repeatability is small. As the measurement was done according to ISO140-3, it is believed that the limitation of this standardized method on the measurement accuracy applies here in the present study. The accuracy of the present measurement should therefore be acceptable.

III. RESULTS AND DISCUSSIONS

There are two possible ways the plenum window can be applied onto a building facade in practice. The first one is the case where the orientation of the building relative to the road traffic is fixed. This usually happens at sites close to the coastline because of view issues. The second one is the case where such building orientation is not restricted. The insertion losses resulting from the installation of the same plenum window in these two cases are different because of the difference in the reference cases. For the fixed building orientation cases, the reference case is the one with opened window and the same orientation angle. For the second one, such reference is provided by the opened window case with $\theta = 0°$ as indicated in Fig. 4. In the latter scenario, the insertion loss is contributed by the plenum window as well as the change in window orientation relative to the source.

A. Fixed building facade orientation

Figure 5 illustrates the variations of the *IL* with the orientation angle θ under various combinations of w and d. The *IL* of the closed window case is also presented for the sake of completeness. For the closed window case, the variation of *IL* is in general symmetrical about $\theta = 0°$, which is expected. Such symmetry further confirms the uniformity of the sound field around the proximity of the scale down model and the latter asymmetry in the angular variation of *IL* for the plenum window cases are the results of the window configurations. The insertion loss decreases with increasing angular deviation from $\theta = 0°$ because of the reduced sound intensity diffracted into the model internal cavity at the window edges as θ deviates away from 0°. The *IL* of ~20 dB of the closed window at $\theta = 0°$ compares well with the real practical range of a single glass pane window,[19] though a bit near to the lower end.

It can be observed from Fig. 5 that the *IL* peaks at approximately the same θ once the plenum depth d is fixed, except for relatively small w. For $w/L = 0.5$, the maximum *IL* appears at the orientation angle $\theta_{max} \sim 15°$. Faster decrease of *IL* is observed as θ approaches $-90°$ than as θ approaches 90°. For negative θ, some sound can go directly into the model cavity through the plenum window, resulting in a relatively large reduction in *IL* (favorable orientation cf. Fig. 3). Some of this direct sound transmission can take place at $\theta \sim 0°$ for this w/L so that the peak *IL* will not appear at this angle. The plenum window oriented at positive θ offers larger resistance to the

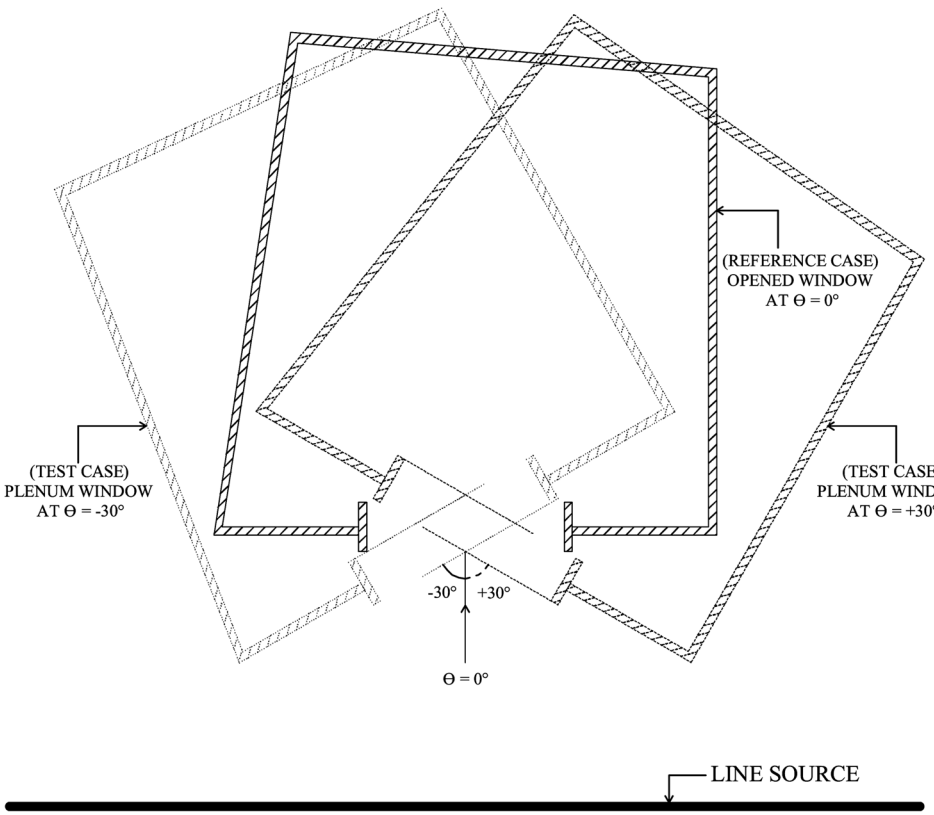

FIG. 4. *IL* calculation reference for the "Unrestricted building facade orientation" cases.

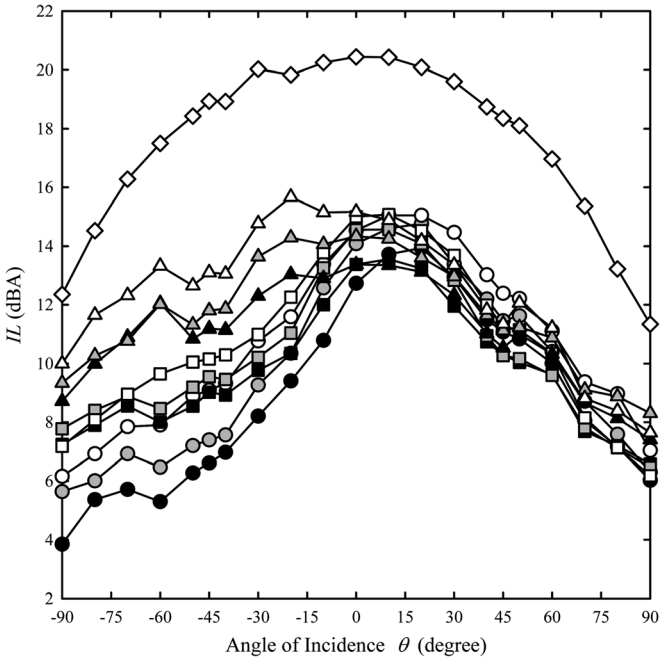

FIG. 5. Angular variation of *IL* for cases with fixed window orientation relative to the line source. $w/L = 0.5$ (open circle); $w/L = 0.25$ (open square); $w/L = 0.1$ (open triangle); window closed (open diamond); Open symbol, $d/L = 0.1$; gray symbol, $d/L = 0.15$; closed symbol, $d/L = 0.2$.

sound transmission which has to be done in the forms of diffraction or indirect reflection mostly. Since the resistance is already large, the reduction of *IL* with increasing θ is slower in such circumstances. At this w/L, the *IL* is reduced at increased d regardless of the angle θ and such reduction is larger for negative θ. This is probably due to the decrease in the magnitude of the acoustic impedance of the plenum window at increased d. For all d studied at this w/L in the present investigation, the rate of decrease of *IL* is slower for $\theta < -45°$. The *IL* of about 12 to 13 dB for the case of $w/L = 0.5$, $d/L = 0.2$ at $\theta = 0°$ is in good agreement with the result of a full scale test conducted inside the authors' laboratory,[20] indicating that the present scaled down model is reasonably reliable.

The decrease of w/L to 0.25 does not change the basic trend of the angular variation of *IL*, except that the variation of *IL* with d is much less significant at this w/L. The angle θ_{max} is between 0° and 10°. One can observe that the *IL*s at large $|\theta|$ are larger than those for $w/L = 0.5$, while those at small θ are not so affected.

The angle of maximum *IL* further shifts towards the negative θ axis as w/L is decreased further to 0.1. At this w/L, θ_{max} appears to be slightly dependent on d. At large d, the *IL*s for $|\theta| < 30°$ are very close. As d is reduced, θ_{max} shows a slight tendency to move to $\sim -20°$. It is noticed that the *IL*s for negative θ increase at a rate faster than those for positive θ as w/L is reduced. Also, the trend of the angular variation of *IL* at $w/L = 0.1$ appears to resemble the opposite of that at $w/L = 0.5$ but is more symmetrical about $\theta = 0°$. At this small window opening situation, the type of direct sound propagation into the model cavity as in the $w/L = 0.5$ case is much less effectively taken place. The large *IL* at negative θ is therefore expected to be the results of higher sound energy loss due to multiple reflections within the plenum window. Since the ways the sound propagates into the model cavity through the plenum window for the negative and positive θ cases are different, the sound protection mechanisms at peak *IL* for the large and small window opening cases are expected to be different. This will be discussed further in Sec. III C.

One can also notice from Fig. 5 that the *IL* for positive θ is nearly an invariant of w when d is fixed. While the *IL* for negative θ increases with decreasing w for all d studied, the rate of increase of the *IL* depends very much on the plenum depth d. For large $d/L = 0.2$, it is found that the *IL*s for $w/L = 0.25$ are somewhat midway between those for $w/L = 0.5$ and 0.1. However, one can observe a rapid increase in *IL* for the case with $d/L = 0.1$ when w/L changes from 0.25 to 0.1. The situation for $d/L = 0.15$ is in the middle.

Figure 6(a) illustrates some examples of the one-third octave band noise reduction R for the cases with $w/L = 0.5$.

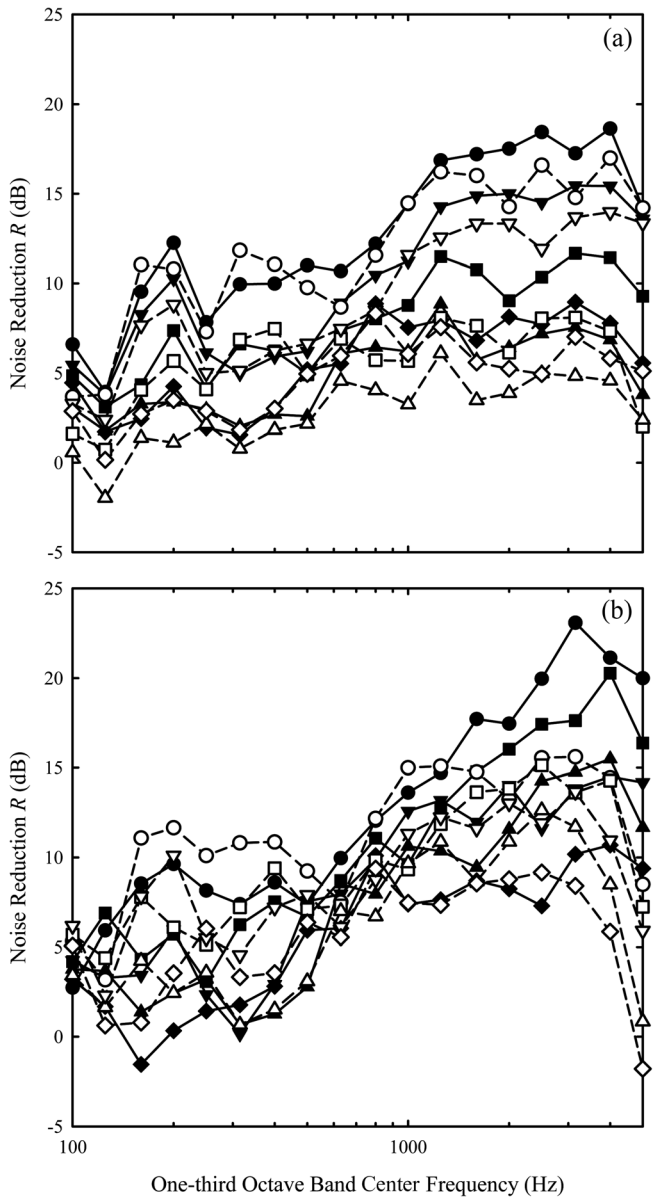

FIG. 6. Examples of one-third octave band sound reduction indices for cases with fixed window orientation relative to the line source. (a) $w/L = 0.5$; (b) $w/L = 0.1$. $\theta = \theta_{max}$ (open circle); $\theta = -45°$ (open square); $\theta = -90°$ (open triangle); $\theta = +45°$ (open inverted triangle); $\theta = +90°$ (open diamond). Open symbol, $d/L = 0.2$; closed symbol, $d/L = 0.1$.

The data show that the noise reduction R increases in general with frequency which is expected and the effect of θ is relatively uniform across the whole frequency range, but with larger increase in R at the higher frequency side of the spectrum probably because of the increased number of sound reflection at smaller d. The trends of frequency variation of R are basically unchanged when d/L varies from 0.1 to 0.2, implying that the acoustic modes associated with the gap separating the window panes are not important. A R peak is observed within the 200 Hz one-third octave band, which is likely to be due to a longitudinal resonance at ~170 Hz along the length of the plenum (to be discussed later). The fluctuation of R appears to be small at frequencies above the 1000 Hz band.

The trend of the frequency variation of R becomes "d sensitive" at $w/L = 0.1$ as shown in Fig. 6(b). For these small window opening cases, only the R at frequencies within the 630 Hz and 800 Hz bands is not significantly affected by changing d. The increase of d appears to enhance the low frequency performance, while that at higher frequencies is reduced. The much narrower sound passage creates greater acoustical energy loss by the multiple reflections than in the cases with $w/L = 0.5$ and thus higher increase in the high frequency performance with decreasing d for negative θ. The relative rapid decrease in R at high frequency (~5000 Hz) is believed to be due to the originally high transmission loss of the high frequency sound (~20 kHz in the experiment). One should also note that the sound field inside the receiver box may not be sufficiently uniform at such a high frequency in the presence of air absorption, resulting in high measurement uncertainty and thus these results are not further discussed. However, this part of the spectrum is not important when the A-weighted traffic noise is the main concern.[14]

Figure 7(a) illustrates some typical average narrow band spectra inside the receiver chamber. It can be observed that there are a number of relatively sharp peaks at frequencies below 150 Hz. The magnitudes of these peaks also appear not affected by the presence of the plenum window not matter what the configuration of the latter is. The very low frequency peaks could be due to the receiver chamber, but are unimportant as the frequency range of the traffic noise as depicted in EN1793-3[14] is from the 100 Hz to 5000 Hz one-third octave band. There is a sound level dip at around 85 Hz in Fig. 7(a). This corresponds to the fundamental longitudinal resonance inside the plenum windows. This resonance also occurs, though not as distinctive as that in the presence of the plenum windows, in the opened window case because of the parallel panel-like model window frames in the present study (cf. Fig. 4). This type of resonance is sharper as the w and d are reduced. The large Rs within the 160 Hz and 200 Hz bands observed in Fig. 6 are the results of the resonance of a harmonic of the abovementioned longitudinal resonance. For the larger w and d case, a relatively broadband reduction is observed because of the much less sharp resonance. The situation becomes very clear in the small w and d case. A sharp dip at around 170 Hz confirms the harmonic resonance.

The narrow band insertion losses for the cases discussed in Fig. 7(a) are presented in Fig. 7(b). One can observe that

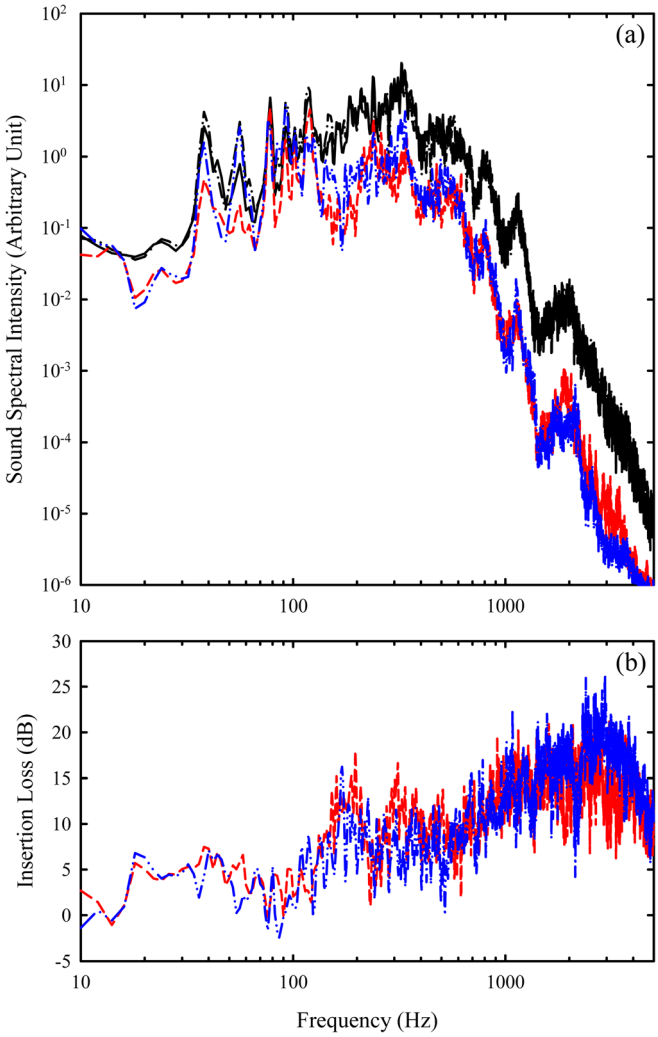

FIG. 7. (Color online) Narrow band sound spectra and insertion losses with a frequency resolution of 2 Hz. (a) Average sound spectra inside the receiver chamber; (b) Insertion loss. Opened window, $\theta = +20°$ (solid line); Opened window, $\theta = -20°$ (dot dashed line); $w/L = 0.5$, $d/L = 0.2$, $\theta = +20°$ (dashed line); $w/L = 0.1$, $d/L = 0.1$, $\theta = -20°$ (double dotted dashed line).

there is also a relatively organized high insertion loss region at frequencies around 300 Hz (260 Hz to ~350 Hz), especially for the larger w and d case. This group of frequencies includes that of the transverse resonance in the plenum window and that of the second harmonic of the plenum longitudinal resonance. As frequency increases further, the insertion loss appears more uniform across each octave band. The individual higher plenum window mode effects are not significant.

B. Unrestricted building facade orientation

When the orientation of the building facade relative to the sound source is unrestricted, the reference for the IL estimation is taken to be the case of opened window with $\theta = 0°$ (Fig. 4). The IL in this case therefore consists of contributions from the plenum window itself and the change in view angle of the source. Figure 8 summarizes the angular variations of IL for the cases investigated. It is not surprising to see the increase of IL under this facade orientation arrangement compared to the data in Fig. 5 due to the reduction of source view. Such increase is small for small θ as expected.

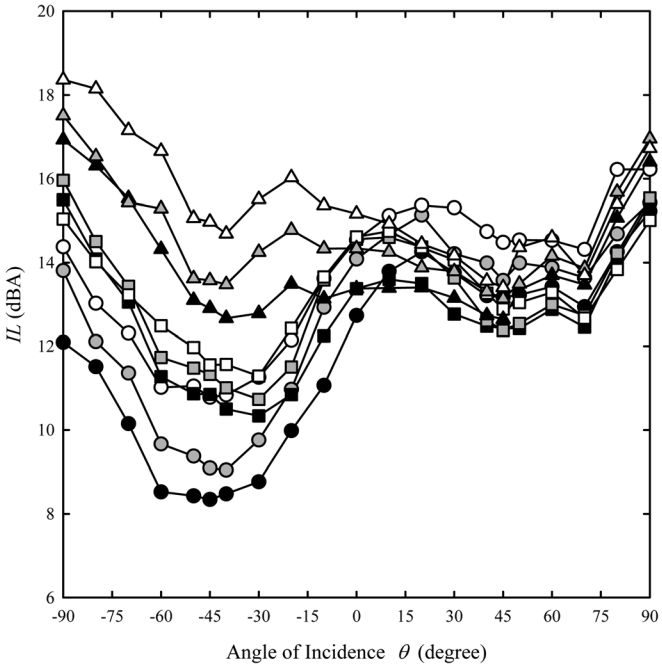

FIG. 8. Angular variation of *IL* for cases for "Unrestricted building facade orientation" cases. Legends are the same as those of Fig. 5.

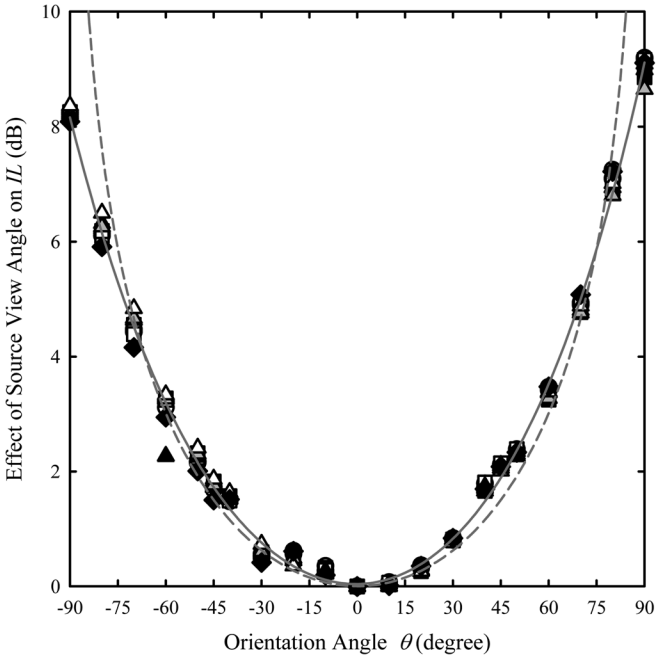

FIG. 9. Effect of source view angle on the *IL*. Regression line (solid line); $\Delta IL = 10\log_{10}|\cos\theta|$ (dashed line). The other legends are the same as those of Fig. 5.

Compared with results in Fig. 5, it is found the variations of *IL* with θ for $|\theta| < 30^{o}$ is not much affected by the change in the source view. For $|\theta| > 45^{o}$ in general, the *IL* increases with increasing $|\theta|$ instead of continuing to decrease as for the case of fixed facade orientation (Fig. 5), suggesting that the effect of source view becomes dominant at larger angles. Minimum acoustical protection is always at $\theta \sim -45°$. In fact, there are small dips of *IL* at $\theta \sim 45°$ due also to the reduction in the source view angle. While the *IL* at $\theta \sim 45°$ is nearly unchanged in the present studied parameter range, that at $\theta \sim -45°$ increases with decreasing *w*/*L*. The difference between the two dips (at $\theta \sim -45°$ and 45°) is thus reduced as *w*/*L* decreases. The much less efficient sound transmission into the model cavity by diffraction for positive θ than the relatively direct sound propagation for negative θ is probably the main reason for the faster increase rate of *IL* with decreasing *w* for $\theta < 0°$ as the latter is more sensitive to sound impedance of the elongated plenum. At small *d* and *w*, the *IL*s at negative θ is comparable to or even higher than those at positive θ. One can again observe from Fig. 8 that the *IL* for $\theta > 10°$ is less sensitive to the change in *d* (cf. Fig. 5). Since the other features of the *IL* variations with fixed *d* are very similar to those presented in Fig. 5, Fig. 8 is not further discussed.

Figure 9 shows the differences between the *IL*s presented in Figs. 5 and 8. These differences indicate the effects of the change in the source view angle on the acoustical insertion loss. The collapse of data for all the cases studied is expected as the angle effect should be independent of the plenum window configurations. This adds to the reliability of the measurement. Also presented in Fig. 9 are the regression line obtained through using a fourth order polynomial and the line $\Delta IL = 10\log_{10}|\cos\theta|$. It is found that the fourth order polynomial gives the best fitting to the current experimental data (Correlation coefficient $R^2 = 0.997$, standard error $\varepsilon = 0.15$ dB) than polynomials of other orders. The line $\Delta IL = 10\log_{10}|\cos\theta|$ indicates the reduction of sound intensity fallen onto the windows due to change in the source view in principle. It is noted that the differences between the two curves and the experimental data are very small for $|\theta| < 70^{o}$. The larger differences observed at $|\theta| > 70^{o}$ are probably due to sound diffraction into the model cavity. This takes place even when the sound is at glazing incidence to the window opening, limiting the value of insertion loss difference as $\theta \to \pm 90°$.

In Fig. 10 are illustrated some examples of the frequency variations of the noise reduction *R*s. It is obvious that the *R*s at $\theta = -45°$ are the lowest, and they are especially low for large *w* at frequencies higher than the 630 Hz band [Fig. 10(a)]. It is no wonder that the *R*s at large $|\theta|$ are basically the highest. The frequency variations of *R*s for the *w*/*L* = 0.5 case are very rough and they are complicated by the effect of orientation which is frequency dependent. The corresponding *R*s for the *w*/*L* = 0.1 case are shown in Fig. 10(b). With the effect of facade orientation included, the *R* appears to increase in principle monotonically with frequency within a band of ~7 dB. *R*s at large $|\theta|$ are also the highest in general. The slope of the *R* increase with frequency appears to increase with decreasing *d*. A *R* peak can still be observed near to the 160 Hz and 200 Hz bands, which is probably the effect of the resonances described in the previous section. Such a peak can also be observed in Fig. 10(a).

Figure 11 summarizes the effects of the facade orientation on frequency variations of the noise reduction ΔR. This is done by subtracting the *R*s in the present cases from those corresponding data presented in the previous section. Since the corresponding data for positive and negative θ are similar, the ΔR presented are the average ones. At small θ, the

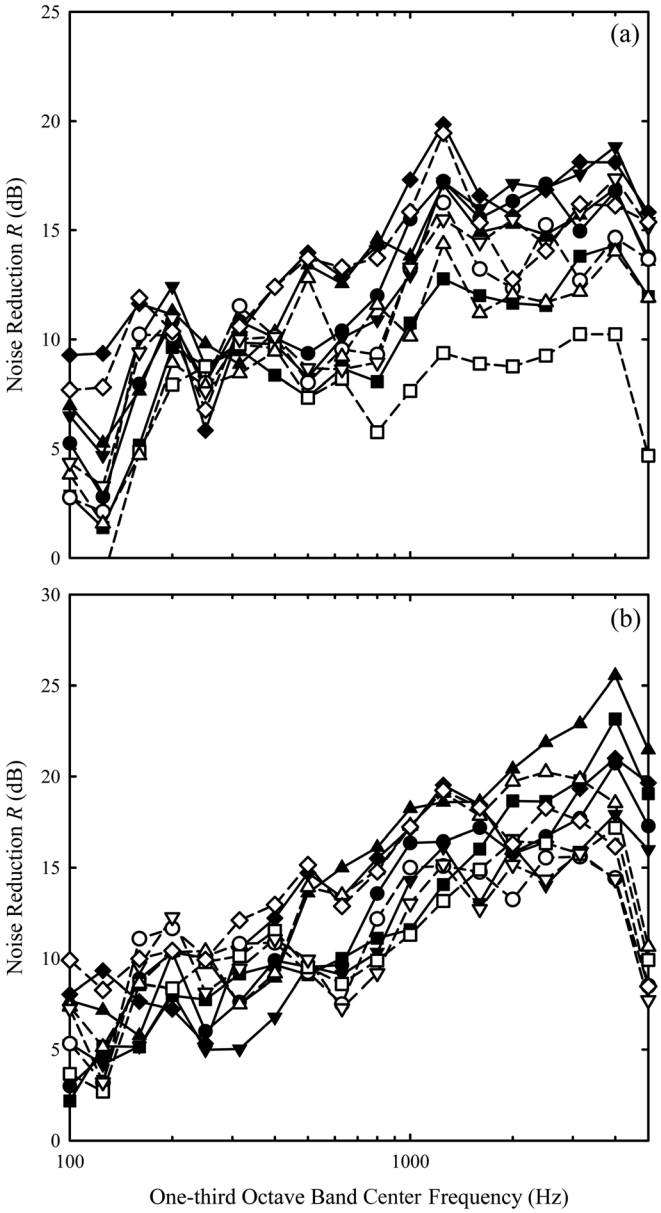

FIG. 10. Examples of one-third octave band noise reduction for "Unrestricted building facade orientation" cases. (a) $w/L = 0.5$; (b) $w/L = 0.1$. The legends are the same as those of Fig. 6, but with θ_{max} defined to be the θ of the highest IL for $|\theta| < 45°$.

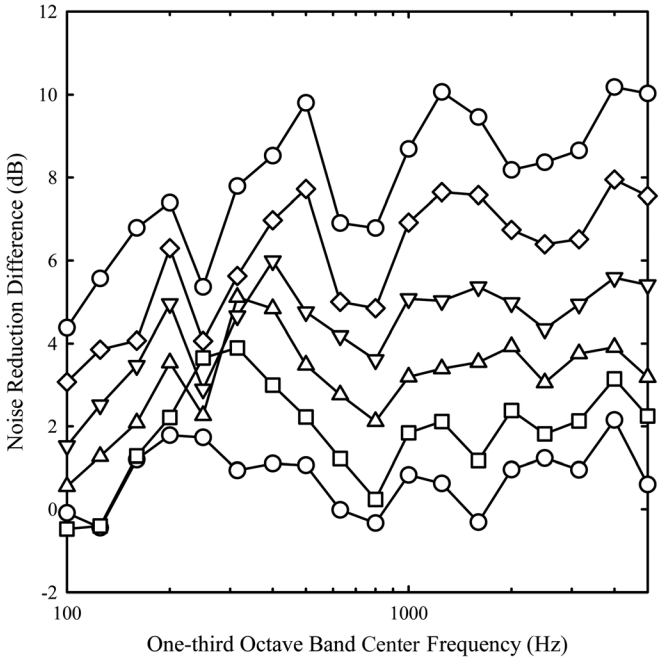

FIG. 11. One-third octave band noise reduction due to facade orientation. $\theta = 30°$ (open circle); $\theta = 45°$ (open square); $\theta = 60°$ (open triangle); $\theta = 70°$ (open inverted triangle); $\theta = 80°$ (open diamond).

contribution of source view angle is just fluctuating within a 2 dB band over the frequency range concerned. When θ is increased to 45°, a relatively fast increase in the ΔR is observed within the 200 Hz to the 500 Hz band. ΔR dips are observed at the 250 Hz and the 2500 Hz band for $\theta \geq 60°$ and the ΔRs at higher frequencies start to rise at a faster rate. It is noted that a ΔR dip can always be observed at the 800 Hz band. The data shown in Fig. 11 are independent of the plenum window configuration and are related to sound diffraction.

C. Numerical simulations

Numerical simulations were performed in an attempt to understand the dynamics of the sound waves when they engaged with the plenum windows. The finite-element method and the wave equation solver implemented by the software COMSOL[21] was used. As the three-dimensional computation is very demanding on computer resources, two-dimensional simulations with anechoic source and receiver regions were carried out instead under the current resource constraint. The outgoing wave boundary condition was adopted at the boundaries of the computation domain, while all the window surfaces and the walls separating the source and receiver regions were rigid. Since the horizontal cross section of the plenum window is more important in the control of sound propagation, the wave dynamics/transmission mechanisms revealed in the present two-dimensional computation are relevant to the scale model study, though an exact comparison is not possible and it is also not the present purpose.

The computations were done on a server with Dual X5650 Xeon Processors (12 cores × 2.66 GHz) and 192 GB memory space. Meshes with at least six elements over a wavelength were set for all regions to ensure the accuracy of calculations. The total number of elements differed from setting to setting, but was kept not less 790 000 and a further refinement of the meshes did not give rise to noticeable differences in the computed results. Full dimensions of the plenum windows (except the height) were used in the computations.

Figure 12 shows the wave mechanics across plenum windows with different w/L and θ while $d/L = 0.2$. The cases without the windows are included for comparison. A mono-frequency line source generating a 1 kHz sound is set at the bottom of each sub-figure. The 1 kHz sound is chosen here for detailed discussion as it and the frequencies around it have the most significant contribution to the A-weighted IL.[14] The sound propagates upward and interacts with the plenum windows. Strong reflection of sound in the source region can be observed unless θ is closed to ±90°. For the opened window cases, standing wave patterns can be

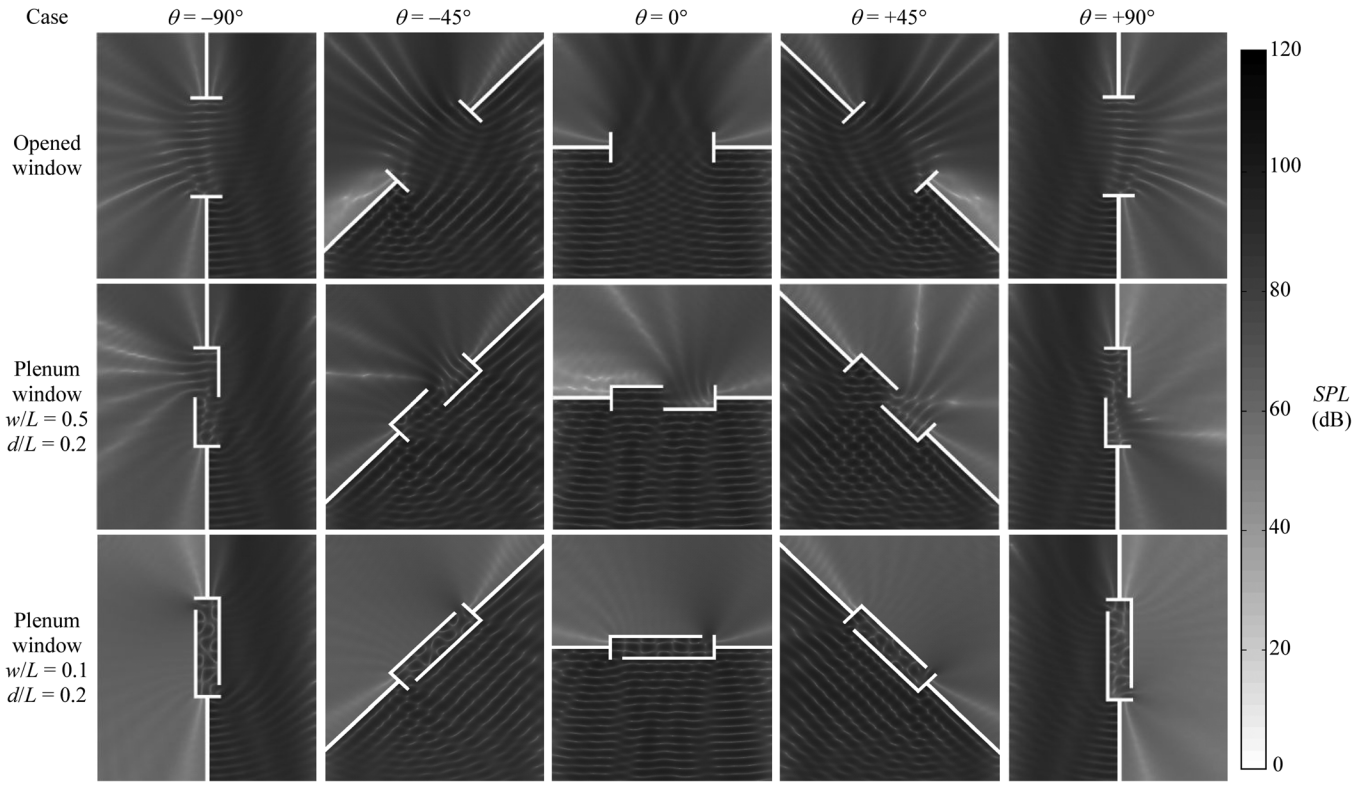

FIG. 12. Examples of simulated sound pressure level distribution maps.

observed, confirming the possibility of longitudinal resonance across the width of the opening.

For the plenum window with $w/L = 0.5$ facing the normal incident sound ($\theta = 0°$), it can be noticed that standing wave pattern parallel to the window pane is observed on the left half of the window, while another standing wave pattern which is parallel to the window side panels is found on the right half of the plenum window cavity. Sound energy is also transmitted from the left half of the window cavity into the receiver region through diffraction. Owing to such diffraction, the orientation of maximum transmission loss θ_{max} for this window configuration will take a slightly positive value as shown in Fig. 5. With the same w/L, the wave dynamics at $\theta = +45°$ are very different from those at $\theta = -45°$. For the case of $\theta = -45°$, one can find the standing wave patterns and diffraction similar to those observed at $\theta = 0°$, except that a stronger standing wave is set up across the width of the window. It is likely that a direct sound transmission across the inclined window has also occurred. Much of the sound energy is reflected back into the source region by the left half of the window at $\theta = +45°$. A much weaker standing wave than that found at $\theta = -45°$ is then created inside the right half of the window cavity as the kind of direct transmission observed in the case of $\theta = -45°$ is not possible. A higher sound transmission loss then follows. This is largely in-line with the results shown in Figs. 5 and 8. Since the reference of the *IL*s presented in Fig. 5 varies with θ and thus the comparison will not be very straight-forward, the results shown in Fig. 8 will mainly be used in the foregoing discussions. Similar phenomenon takes place at glazing incidence ($\theta = \pm 90°$). Again direct sound transmission is likely for ($\theta = -90°$), resulting in lower insertion loss compared to its ($\theta = +90°$) counterpart.

The bottom two rows of sound pressure level maps in Fig. 12 illustrate the effect of reducing w/L on the wave dynamics. The reduction of w/L from 0.5 to 0.1 does reduce significantly the amount of sound energy that can enter the window cavity. As direct sound transmission is no longer possible under this configuration and the sound intensities reaching the inlets of the windows inclined at $\theta = -45°$ and $\theta = +45°$ are very similar, the difference between the *IL*s with $\theta = -45°$ and $\theta = +45°$ is small. This applies to all other values of θ. This is also in-line with the scale model experimental results shown in Fig. 8. One can observe that the sound field inside the window cavity is dominated by strong higher acoustic modes at this small w when forced by a 1 kHz sound. The effects of reducing d/L on the wave dynamics are very similar to those of reducing w/L and thus they are not presented.

IV. CONCLUSIONS

A scale down model experiment was conducted in a semi-anechoic chamber in the present study in order to understand the acoustical insertion losses of plenum windows in the presence of a line source. The line source was made up of twenty-five 6 in. aperture loudspeakers. The effects of the orientation of the line source relative to the plenum window normal and those of the window configurations on the insertion loss were also investigated. The overall size of the window void was 500 mm (wide) by 250 mm (high). With a scale down ratio of 1:4, this window corresponded to

a window void of 2 m by 1 m in the practical scenario. Apart from narrowband data, the normalized traffic noise spectrum was used in order to understand the A-weighted traffic noise attenuations provided by the plenum windows. Numerical simulation was also performed for better understanding of the physical mechanisms of the sound transmission. Owing to the configuration of the plenum window, there is a window orientation which favors direct sound propagation across the window and this has been confirmed by the numerical results.

Two types of insertion losses are introduced in the present study. The first one is for the case where the building facade orientation is fixed relative to the traffic. The reference case for the insertion loss estimation is the fully opened window. Under this circumstance, the A-weighted traffic noise insertion loss is the highest when the line source is making a small angle with the model facade. This insertion loss decreases quickly when this angle increases. When the window orientation is in the abovementioned "favorable" propagation condition, such reduction in insertion loss is less rapid when the window opening becomes smaller or when the plenum gap becomes narrower. The insertion loss appears not sensitive to the change in window configuration when the window orientation is not in the "favorable" propagation condition. The maximum insertion loss achieved in the present study is around 14 dB. The minimum insertion loss is found where the line source is in a direction perpendicular to the plenum window. A 4 to 6 dB traffic noise insertion loss is recorded in such cases.

The second type of insertion loss is for the case where the building facade orientation relative to the traffic can be changed. In this case, the reference case for the insertion loss is taken to be the one when the building facade is parallel to the traffic and the window is fully opened. The insertion loss so estimated therefore consists of the effects of the plenum window as well as the source orientation. The maximum traffic noise insertion loss appears when the line source is in a direction perpendicular to the plenum window (opposite to the previous case). A 18 dB insertion loss can be achieved using the studied plenum window configurations. Minimum traffic noise insertion loss recorded is $\sim$8 dB and is found when the line source is making an angle of 45° with the window normal when the window orientation is in the "favorable" propagation condition. Again, the insertion loss is much less sensitive to the change in window configuration when the window orientation is not in the "favorable" propagation condition.

The narrowband data suggest some lower order plenum acoustic modes are affecting the insertion losses of the plenum windows, resulting in high insertion losses at the low frequency side of the spectrum regardless the type of insertion loss concerned. Such effect becomes sharper when both the window opening and the plenum depth become smaller.

The present study is focused on the acoustical insertion losses of plenum windows at different orientations relative to a sound source made up of a long linear loudspeaker array. The effects of other parameters, such as the reverberations inside the receiver room and the elevation of the window from the sound source, on the plenum window insertion loss are still unclear and are left to further investigations.

ACKNOWLEDGMENT

Y.G.T is supported by a scholarship from the Ministry of Higher Education, Malaysia.

[1]Environmental Protection Department, *A Comprehensive Plan to Tackle Road Traffic Noise in Hong Kong* (HKSAR Government, Hong Kong, 2006), p. 14.
[2]K. M. Li and S. H. Tang, "The predicted barrier effects in the proximity of tall buildings," J. Acoust. Soc. Am. **114**, 821–832 (2003).
[3]S. K. Tang, "Noise screening effects of balconies on a building facade," J. Acoust. Soc. Am. **118**, 213–221 (2005).
[4]A. J. B. Tadeu and D. M. R. Mateus, "Sound transmission through single, double and triple glazing. Experimental evaluation," Appl. Acoust. **62**, 307–325 (2001).
[5]A. Jakob and M. Möser, "Active control of double-glazed windows, Part I & II," Appl. Acoust. **64**, 163–196 (2003).
[6]M. H. F. de Salis, D. J. Oldham and S. Sharples, "Noise control strategies for naturally ventilated buildings," Build. Environ. **37**, 471–484 (2002).
[7]I. Sharland, *Wood's Practical Guide to Noise Control* (Woods Acoustics, Colchester, England, 1979), pp. 90.
[8]F. Cotana, "Experimental data and performances of new high sound insulation ventilating windows," *Proc. Inter-noise 1999*, Florida, pp. 995–998.
[9]A. Lawrence and M. Burgess, "Traffic noise and the open window," J. Acoust. Soc. Am. **72**, S91 (1982).
[10]R. D. Ford and G. Kerry, "The sound insulation of partially open double glazing," Appl. Acoust. **6**, 57–72 (1973).
[11]J. Kang and M. W. Brocklesby, "Feasibility of applying micro-perforated absorbers in acoustic window systems," Appl. Acoust. **66**, 669–689 (2005).
[12]UK Department of Transport, *Calculation of Road Traffic Noise* (U.K. Department of Transportation, London, 1988), pp. 10–29.
[13]DIRAC, *Dual Input Room Acoustics Calculator User Manual* (Acoustics Engineering, Denmark, 2002), pp. 17–19.
[14]BS EN 1793-3, *Road Traffic Noise Reducing Devices—Test Methods for Determining the Acoustic Performance—Part 3. Normalized Traffic Noise Spectrum* (ISO, London, 1998).
[15]BS EN ISO 140-3, *Acoustics—Measurement of Sound Insulation in Buildings and of Building Elements—Part 3: Laboratory Measurements of Airborne Sound Insulation of Building Elements* (BSI, London, 1995).
[16]J. Kang, "An acoustic window system with optimum ventilation and daylighting performance," Noise Vib. Worldwide **37**, 9–17 (2006).
[17]M. Garai and P. Guidorzi, "European methodology for testing the airborne sound insulation characteristics of noise barriers in situ: Experimental verification and comparison with laboratory data," J. Acoust. Soc. Am. **108**, 1054–1067 (2000).
[18]C. Buretti, "Indoor noise reduction index with open window," Appl. Acoust. **63**, 431–451 (2002).
[19]BS 8233, *Sound Insulation and Noise Reduction for Buildings—Code of Practice* (BSI, Geneva, Switzerland, 1999).
[20]Environ, *Technical Report on the Acoustic Performance Evaluation of the Special Window* (Housing Department, HKSAR Government, Hong Kong, 2009), pp. 5–6.
[21]COMSOL Multiphisycs, *Acoustics Module User's Guide* (COMSOL AB, Sweden, 2008).